European Journal of Engineering and Applied Sciences

ISSN: 2651-3412 (Print) & 2667-8454 (Online)
Journal homepage: http://dergipark.gov.tr/EJEAS
Published by Çorlu Faculty of Engineering, Tekirdağ Namık Kemal University

European J. Eng. App. Sci. 8(1), 24-30, 2025

Research Article

Compact Microstrip-Coupled Ring Resonator for Angular Displacement Detection

Nazli Merve Tezel[1,a], Merve Efe[1,b], Sena Esen Bayer Keskin[2,c,*], Nurhan Turker Tokan[1,d]

[1]Department of Electronics and Communication Engineering, Faculty of Electrical and Electronics Engineering, Yildiz Technical University, Istanbul, Türkiye, 34220
[2]Department of Electrical Electronics Engineering, Faculty of Engineering, Kırklareli University, Kırklareli, Türkiye, 39100
[a]merve.tezel@std.yildiz.edu.tr, [b]merve.efe1@std.yildiz.edu.tr, [c]senakeskin@klu.edu.tr , [d]nturker@yildiz.edu.tr

Received: 22.05.2025 Accepted: 19.06.2025 DOI: 10.55581/ejeas.1704369

Abstract: In this work, a planar microwave angular displacement sensor featuring concentric and precisely aligned stator and rotor components for accurate angular position measurement is presented. The sensor operates using a dual-band architecture incorporating two concentric loop resonators to enhance angular sensing performance. The structure is realized on two FR-4 printed circuit boards (PCBs), each measuring 40 mm × 40 mm with a thickness of 1.6 mm. The PCBs are arranged such that the conductive layers containing the microstrip patterns face each other, ensuring strong electromagnetic coupling and precise concentric alignment**.** The rotor consists of a split-ring resonator patterned on the underside of the upper PCB and is placed concentrically within a circular aperture on the top layer**.** The stator comprises all regions outside the circular apertures on both PCBs. The lower PCB includes a straight microstrip feed line magnetically coupled to a closed-loop primary resonator**.** The split-ring resonator on the rotor is positioned directly above the primary resonator, facilitating strong mutual coupling. Simulation results indicate resonances at 2.17 GHz and 3.57 GHz, demonstrating dynamic angular sensing capability over a 0° to 90° rotation range. Full-wave electromagnetic simulations reveal absolute angular sensitivities of 0.83 MHz/° and 0.40 MHz/° at the respective resonant frequencies. The findings indicate that the proposed sensor design holds significant potential for industrial applications requiring precise angular displacement measurements.

Keywords: *Microwave sensor, Angular displacement sensor, Split ring resonator, Resonant frequency.*

Açısal Sapma Kontrolü için Mikroşerit İletim Hattı Kuplajlı Halka Rezonatör Tasarımı

Öz. Bu çalışmada**,** doğru açısal konum ölçümü sağlayan, eş merkezli olarak hizalanmış stator ve rotor bileşenlerine sahip düzlemsel bir mikrodalga açısal yer değiştirme sensörü sunulmaktadır. Sensör, iki eş merkezli halka rezonatör içeren çift bantlı bir mimariyle çalışarak açısal algılama performansını artırmaktadır. Yapı, her biri 40 mm × 40 mm boyutlarında ve 1.6 mm kalınlığında iki FR-4 baskılı devre kartı (PCB) üzerine gerçekleştirilmiştir. PCB'ler, üzerlerindeki iletken desenleri içeren katmanlar (yani mikroşerit yapıların bulunduğu yüzeyler) birbirine bakacak şekilde konumlandırılarak, güçlü elektromanyetik etkileşim ile doğru eş merkezli hizalama sağlanmaktadır. Rotor, üst PCB'nin alt yüzeyine desenlenmiş bir yarıklı halka rezonatörden oluşmakta olup, üst katmandaki dairesel boşluğa eş merkezli biçimde yerleştirilmektedir. Stator ise her iki PCB'nin dairesel açıklık dışındaki bölgelerinden oluşmakta; alt PCB üzerinde yer alan doğrusal mikroşerit iletim hattı**,** kapalı halka biçimindeki bir birincil rezonatör ile manyetik olarak bağlanmaktadır. Rotor üzerindeki yarıklı halka rezonatör, bu birincil rezonatörün tam üzerinde konumlanarak güçlü karşılıklı etkileşim sağlamaktadır. Simülasyon sonuçları, sensörün 2.17 GHz ile 3.57 GHz frekanslarında rezonans yaptığını ve 0° ile 90° arasında dinamik bir açısal algılama gerçekleştirebildiğini göstermektedir. Tam dalga elektromanyetik benzetim sonuçları, bu rezonanslarda sırasıyla 0.83 MHz/° ve 0.40 MHz/° mutlak açısal hassasiyet sunduğunu ortaya koymaktadır. Elde edilen bulgular, önerilen sensör yapısının, hassas açısal yer değiştirme ölçümü gerektiren endüstriyel ortamlar için yüksek potansiyele sahip olduğunu göstermektedir.

Anahtar kelimeler*: Mikrodalga sensör, Açısal yer değiştirme sensörü, Yarık halka rezonatör, Rezonans frekansı*

* Corresponding author
E-mail address: senakeskin@klu.edu.tr (S. E. Bayer Keskin)

1. Introduction

Microwave sensors are widely utilized in present-day research due to their ease of fabrication and design, cost-effectiveness, and their ability to provide solutions for a variety of industrial applications. These sensors are designed based on different principles to measure various physical qualities and quantities. Microwave sensors can be employed for determining the angular position or distance of an object relative to the sensor [1], for precise humidity measurements [2], material characterization [3], detection of structural defects in materials [4], as well as temperature [5] and pressure [6] measurements. They are also used in biomedical applications for investigating structural changes in tissues [7], and in scenarios where physical contact is not possible or desirable. Depending on the application, microwave sensors exhibit significant diversity. Some notable types include complementary split ring resonator (CSRR)-based sensors [8], microstrip line split ring resonator (SRR)-based sensors [9], metamaterial-based sensors [10], multi-mode resonator (MMR) sensors [11], SRR-based sensors utilizing cross-polarized excitation [12], and directional coupler-based sensors [13]. These sensors can offer wide dynamic ranges, such as 0°–90°, 0°–180°, or even up to 360°, depending on the specific application [14]. Microwave angular-displacement sensors reported in the literature can generally be grouped into three categories: (i) amplitude-based, (ii) phase-based, and (iii) frequency-shift-based sensors. An amplitude-modulated microwave angular-displacement antenna aimed at chipless RFID applications was proposed in [15]. Reference [16] described a rotary sensor whose operation relies on changes in the phase difference of the reflection coefficients. Nonetheless, owing to its superior reliability and robustness, frequency-shift interrogation has become the most widely adopted technique for microwave angular sensors **[**17**].** The sensitivity of microwave rotational (angular displacement) sensors can vary depending on several factors. In sensor design, criteria such as the physical dimensions of the sensor, the desired operating frequency, and the target angular measurement range are of particular importance. Design parameters are determined with these considerations in mind. Parameters such as the electrical properties of the substrate material, the physical dimensions of the rings, and the stator–rotor (or rotor) separation are also critical. During the design process, these parameters must be carefully selected to achieve the desired sensitivity and dynamic range characteristics. The dynamic sensing range is a critical characteristic that defines the performance of microwave sensors. Various dynamic ranges have been reported for different sensor designs. For instance, while the dynamic range of angular displacement sensors was limited to approximately 6°–8° in earlier studies [18]**,** advancements in design have led to the reporting of microwave sensors with wider ranges in more recent literature. In particular, some planar microwave angular displacement sensors based on microstrip line split-ring resonators (SRRs) have achieved a full 360-degree dynamic range [19]. Overall, microwave sensors have been shown to offer broader dynamic ranges compared to traditional sensors, making them advantageous for a variety of applications [20**,** 21].

In this work, a microwave resonator-based angular displacement sensor was designed to determine the angle of rotation. The proposed microwave split-ring resonator sensor operates within a dynamic detection range of ±90 degrees and, due to its simple structure, offers ease of fabrication and low production cost. The sensor consists of two loop resonators. The use of two concentric ring structures generates two distinct resonance frequencies, thereby enhancing the sensitivity of the sensor. This dual-frequency configuration enables the sensor to respond more sensitively to small angular variations.

2. Design and Parametric Analysis

A dual ring resonator structure, operating in conjunction with a straight microstrip transmission line, is employed to design the planar microwave angular displacement sensor. The printed circuit board (PCB) substrate is made of FR4 material with a thickness of 1.6 mm. The dielectric constant of the substrate is 4.3, and the conductive material is copper with a conductivity of $\sigma = 5.8 \times 10^7$ S/m. The width of the microstrip transmission line, which is used in a straight configuration between the input and output ports, is adjusted to achieve a characteristic impedance of 50 Ω. The coupling strength between the ring resonator and the transmission line is controlled by adjusting the distance between them. The top and perspective views of the designed microstrip transmission-line-coupled ring resonator are shown in Figure 1. As illustrated, the angular displacement sensor consists of stator and rotor sections. The stator comprises the lower PCB and the fixed upper PCB, while the rotor consists of the inner ring of the dual ring resonator and the rotating substrate.

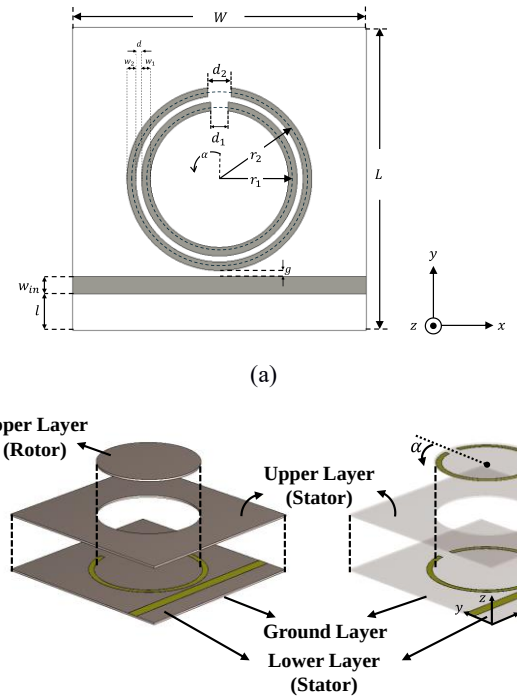

Figure 1. *Microstrip transmission-line-coupled ring resonator: (a) top view; (b) perspective view*

The rotor consists of a rotatable slotted ring resonator (RSRR) structure designed on a circular substrate. This structure is positioned within the circular window located in the stator section, enabling electromagnetic coupling with the primary split ring resonator (PSRR). Both layers are fabricated from FR-4 material, each with a thickness of 1.6 mm and a dielectric constant of 4.3. The parameters of the sensor are provided in Table 1. Here, W denotes the width of the substrate, L is the length of the substrate, win is the width of the feed line, l is the distance between the feed line and the lower edge of the PCB, g is the distance between the lower end of the primary ring and the upper end of the feed line, r_1 and r_2 are the inner and outer radii of the rings, d_1 and d_2 are the slot widths of the inner and outer rings, w_1 and w_2 are the thicknesses of the rings, and d is the spacing between the rings.

2.1. Parametric Analysis

In this section, the effects of variations of the design parameters on the resonance will be examined. The influence of critical physical parameters on the resonance frequencies will be discussed. The term "primary ring" will refer to the outer ring with the larger radius, while "secondary ring" will denote the inner split ring with the smaller radius.

Figure 2 analyzes the effect of the distance between the microstrip transmission-line-coupled ring resonator and the feed line on angular displacement control. The parameter g represents the distance between the upper end of the feed line and the lower end of the primary ring. As seen in Figure 2, when the primary ring resonator structures are in contact with the feed line, the frequency response of the dual-ring resonator sensor exhibits two distinct resonance points. As long as the feed line remains in contact with the rings, the resonance behavior persists**,** with the resonance frequencies shifting toward higher frequency regions in the spectrum depending on the distance. When the physical connection between the feed line and the resonator rings is removed, almost no resonance behavior is observed. Based on the obtained data, the value of the g parameter was selected as 0.5 mm along the negative y direction, corresponding to the case where the two lines are in contact.

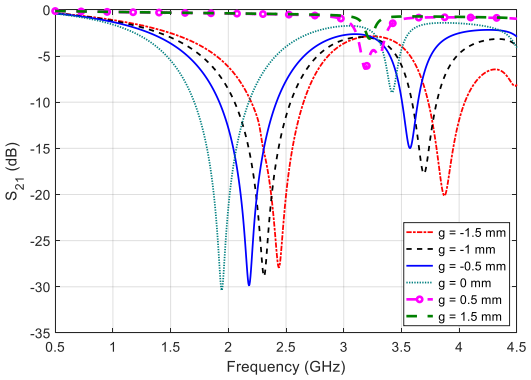

Figure 2. *Effect of the g parameter on the transmission coefficient in the microstrip transmission-line-coupled ring resonator sensor*

Figure 3 illustrates the impact of the parameter r_1 — defined as the radius of the virtual circle connecting the centers of the rings and the midpoint of the secondary ring—on the transmission coefficient of the microstrip transmission-line-coupled ring resonator sensor. While the radius of the primary ring remains fixed**,** increasing the radius of the secondary split ring exhibits negligible effect on the first resonance region. However, noticeable distortions emerge in the second resonance region.

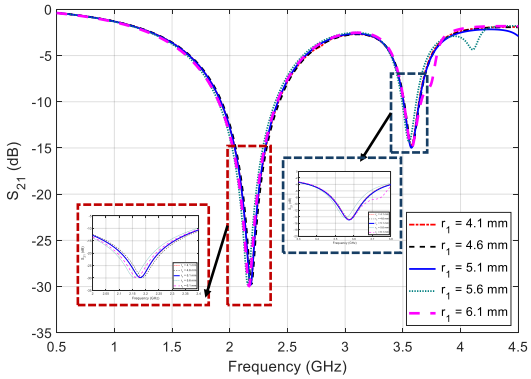

Figure 3. *Effect of the r_1 parameter on the transmission coefficient in the microstrip transmission-line-coupled ring resonator sensor*

Figure 4 analyzes the effect of the r_2 parameter—defined as the radius of the virtual circle between the centers of the rings and the midpoint of the primary ring—on the transmission coefficient in the microstrip transmission-line-coupled ring resonator sensor**.** While the radius of the secondary split ring is kept constant, the radius of the primary ring is varied**.** In the simulation, r_2 ranges from 6.1 mm to 8.1 mm**.** When r_2 is set to 6.1 mm, no resonance behavior is observed in the first frequency region**.** This outcome resembles the case in the g parameter analysis in Figure 3, where g = 0.5 mm along the negative y-axis. It is inferred that insufficient coupling occurs when a gap exists between the feed line and the resonator rings. Consequently, r_2 = 7.1 mm was chosen as the optimal value, providing adequate S_{21} levels at both resonance frequencies**.**

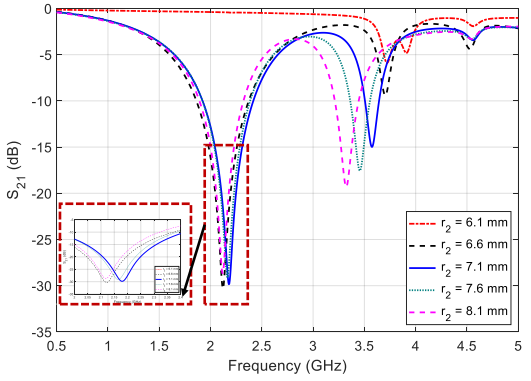

Figure 4. *Effect of the r_2 parameter on the transmission coefficient in the microstrip transmission-line-coupled ring resonator sensor*

Figure 5 illustrates the influence of the parameter d_1, defined as the slot width of the secondary ring, on the transmission coefficient of the microstrip-coupled ring resonator sensor**.** Based on angular displacement analyses, a d_1 value of 1.5 mm was determined to yield high angular stability. Figure 6 presents the effect of the d_2 parameter—defined as the slot width of the primary ring—on the transmission coefficient. As shown in the figure, the optimal value for d_2 was selected as 0 mm, corresponding to a fully closed primary ring.

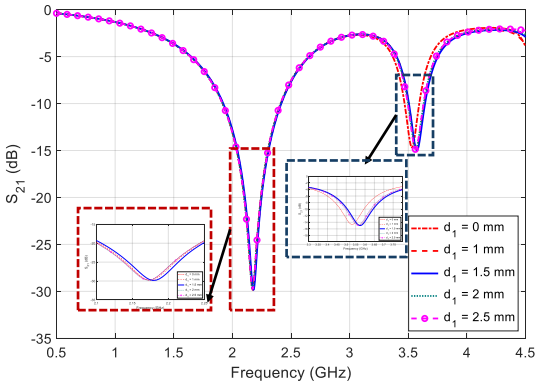

Figure 5. Effect of the d_1 parameter on the transmission coefficient in the microstrip transmission-line-coupled ring resonator sensor

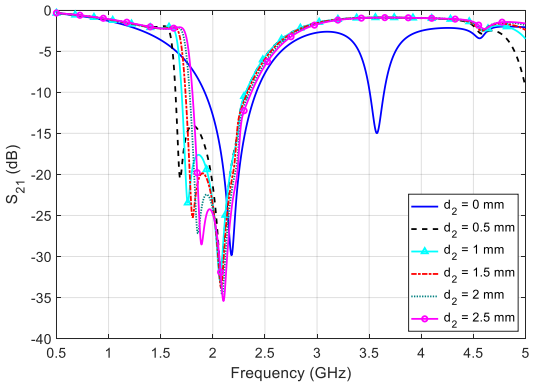

Figure 6. *Effect of the d_2 parameter on the transmission coefficient in the microstrip transmission-line-coupled ring resonator sensor*

Figure 7 illustrates the effect of the w_1 parameter—defined as the width of the secondary split ring—on the transmission coefficient of the resonator. In this analysis, the thickness of the secondary ring was varied while maintaining a constant spacing d between the primary and secondary rings**.** As observed in Figure 7, increasing the w_1 value leads to a downward shift in the second resonance frequency.

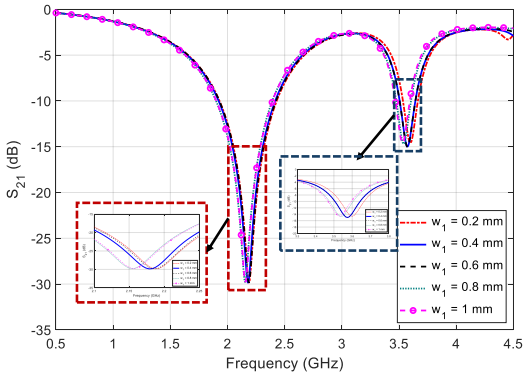

Figure 7. *Effect of the w_1 parameter on the transmission coefficient in the microstrip transmission-line-coupled ring resonator sensor*

Figure 8 presents the effect of the w_2 parameter-defined as the width of the outer (primary) ring-on the transmission coefficient of the resonator. In this analysis, the thickness of the primary ring was varied while keeping the distance d between the two rings constant. As shown in the figure, an increase in w_2 results in a higher first resonance frequency and a reduction in the S_{21} level to approximately –32 dB. In the second resonance region, both the resonance frequency and the S_{21} level increase with increasing w_2, reaching up to –14 dB.

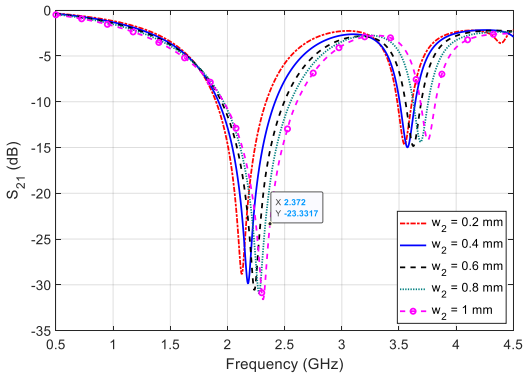

Figure 8. *Effect of the w_2 parameter on the transmission coefficient in the microstrip transmission-line-coupled ring*

After the parametric analysis, the parameter values are selected as follows: W = 40 mm, L = 40 mm, l = 13 mm, r_1 = 5.1 mm, r_2 = 7.1 mm, w_1 = w_2 = 0.4 mm, d_1 = 1.5 mm, d_2 = 0 mm, and g = –0.5 mm. The overall dimensions of the sensor are 40 mm × 40 mm. The physical dimensions of the sensor are listed in Table 1.

Table 1 Dimensions of the microstrip transmission-line-coupled ring resonator

Parameter	Dimension (mm)	Parameter	Dimension (mm)
W	40	r_2	7.1
L	40	d_1	1.5
w_{in}	2.45	d_2	0
l	13	w_1	0.4
g	-0.5	w_2	0.4
r_1	5.1	d	1.6

2.2. Final Design

Due to the presence of two ring structures, it is expected that the design exhibits resonance at two distinct frequencies. The views of the microstrip transmission-line-coupled ring resonator sensor in the simulation software are presented in Figure 9. Figure 9 (a) shows the top view of the lower PCB, which corresponds to the stator section. Figure 9 (b) presents the bottom view of the upper PCB, where the ring structure is referred to as the rotor. The stator is a fixed structure and forms a complete assembly with the rotor. Angular displacement can be detected by monitoring changes in the resonance frequency regions. Figure 9 (c) illustrates the top perspective view of the structure. Figure 9 (d) displays the top view of the microwave resonator sensor, equipped with connectors and ready for fabrication.

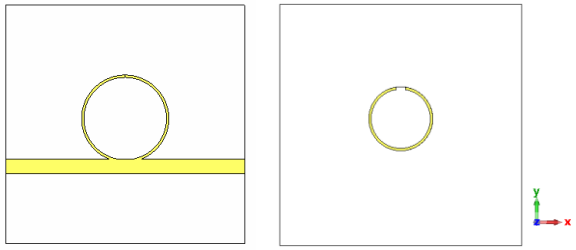

(a) (b)

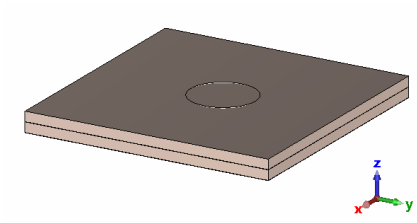

(c)

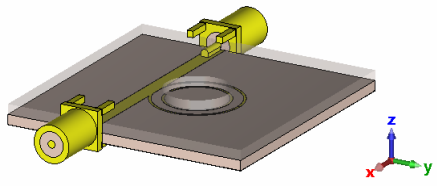

(d)

Figure 9. *Simulated views of the microstrip transmission-line-coupled ring resonator: (a) top view of the lower PCB; (b) bottom view of the upper PCB; (c) perspective view; (d) top view of the microwave resonator with connectors*

Figure 10 illustrates the frequency-dependent behavior of the microstrip transmission-line-coupled ring resonator for angular displacement control**,** presenting the transmission and reflection characteristics of the dual-ring microwave resonator**.** The first resonance is observed at 2.17 GHz, accompanied by a return loss of approximately 30 dB. The second resonance occurs at 3.57 GHz, with a corresponding return loss of about 15 dB**.** These results correspond to an angular displacement of α=0°.

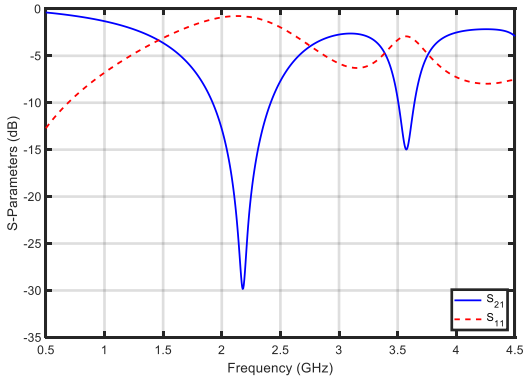

Figure 10. *S-parameters of the microstrip transmission-line-coupled ring resonator*

Figure 11 presents the surface current distribution of the microstrip transmission-line-coupled ring resonator at its resonance frequencies**.** In Figure 11(a), the distribution at 2.17 GHz is shown, where the maximum surface current density reaches 72.7 A/m. At this frequency, due to the resonant behavior, the signal transmitted to the second port is significantly attenuated**.** Similarly, Figure 11(b) illustrates the distribution at 3.57 GHz, where the maximum current density increases to 108 A/m, exhibiting a resonance pattern comparable to that observed at the first resonance frequency**.**

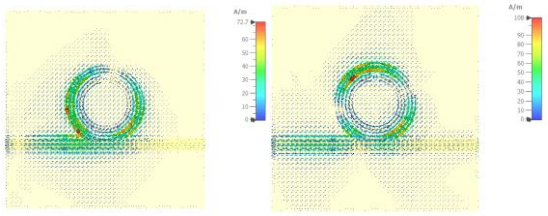

(a) (b)

Figure 11. *Surface current distributions at the resonance frequencies of the microstrip transmission-line-coupled ring resonator: (a) 2.17 GHz; (b) 3.57 GHz*

3. Microstrip-Coupled Ring Resonator for Angular Displacement Detection

This section examines the microstrip-coupled ring resonator's transmission and reflection behavior as the function of angular displacement. Frequency shifts observed between α = 0° and 90° demonstrate the sensor's sensitivity to rotation. Coupling effects between the rings influence resonance characteristics, enabling precise angular position detection.

Figure 12 analyzes the reflection and transmission parameters of the microwave resonator at angular positions $\alpha = 0°$ and $\alpha = 90°$. At $\alpha = 0°$, two distinct resonance notches are observed, while at $\alpha = 90°$, an additional dip emerges near the first resonance frequency. This distortion is likely caused by coupling between the slot region of the secondary ring and the feed line as the rotor structure rotates.

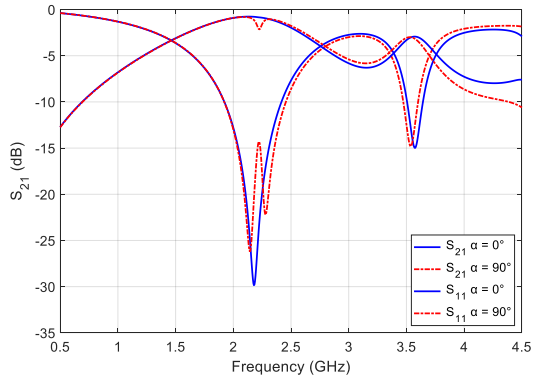

Figure 12. *Frequency-dependent variation of the S-parameters for $\alpha = 0°$ and $\alpha = 90°$*

Figure 13 shows the simulated S_{21} characteristics of the sensor as the rotor is rotated counter-clockwise from $\alpha = 0°$ to $\alpha = 90°$ with 15° increments. The resonance frequency f_1, originating from the primary split ring resonator (PSRR), decreases approximately linearly from 2.17 GHz to 2.14 GHz. The first and second resonance regions are clearly visible in the resulting graph. The resonance frequency f_2, originating from the secondary SRR, varies between 3.57 GHz and 3.54 GHz. As the angle increases, the frequency decreases, enabling the detection of angular displacement.

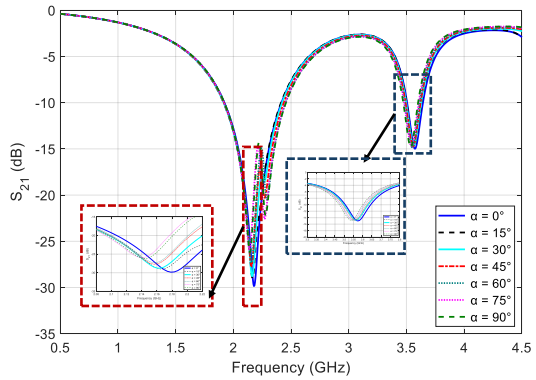

Figure 13. *Frequency dependence of the transmission coefficient for different α values in the ring resonator sensor*

Absolute sensitivity (S_{abs}) and relative sensitivity (S_{rel}) are important parameters used to assess the performance of microwave angular displacement sensors. S_{abs} is defined as the ratio of the change in resonance frequency ($f_a - f_b$) to the change in angular displacement ($\Delta\theta$), where f_a and f_b represent the maximum and minimum resonance frequencies, respectively, over the frequency shift range. Relative sensitivity is obtained by normalizing this frequency shift with respect to the initial resonance frequency and expressing the result as a percentage per degree as given in Eq.2:

$$S_{abs} = (f_a - f_b) \cdot \frac{1}{\Delta\theta} \qquad (1)$$

$$S_{rel} = (f_a - f_b) \cdot \frac{1}{\Delta\theta} \cdot 100\,\% \qquad (2)$$

Based on Equations (1) and (2), S_{abs} for the f_1 resonance band is calculated as 0.03 MHz/°, and S_{rel} as 0.001 % /°. For the f_2 resonance band, the absolute and relative sensitivities are determined as 0.40 MHz/° and 0.01 %/°, respectively.

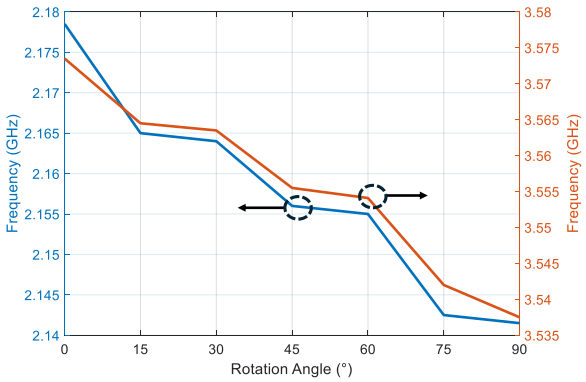

Figure 14. *Relationship between the alpha angle and the primary ring resonance frequencies of the microwave resonator sensor*

Figures 14 and 15 illustrate the influence of the angular displacement α on the resonator's performance. Figure 14 shows the resonance frequency shifts of the primary (blue) and secondary (orange) rings, while Figure 15 displays the corresponding transmission losses at these frequencies as a function of α. Figure 15 presents the variation of the resonance frequencies f_1 and f_2 as a function of the angular displacement α in the range of 0° to 90°.

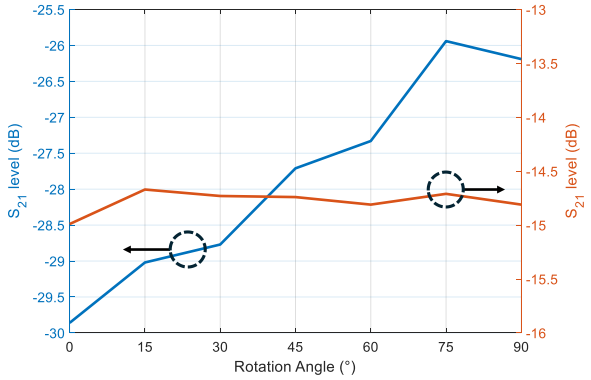

Figure 15. *Relationship between the alpha angle and the transmission loss levels at the first (blue) and second (orange) resonance frequencies of the microwave resonator sensor*

4. Conclusion

In this study, a microwave angular displacement sensor with a dynamic detection range of ±90° is presented. The proposed sensor features a compact footprint of 40 mm × 40 mm. The effects of design parameters on the operating frequency and angular response of the sensor have been systematically analyzed. Future work may involve the development of alternative configurations with varied dimensions and expanded application domains. Due to its compactness and ease of design and manufacturability, the proposed sensor provides a practical and reliable solution for angular displacement measurements.

Author Contribution

Conceptualization, N.M.T. (Nazlı Merve TEZEL); Data curation, N.M.T. and N.T.T. (Nurhan TÜRKER TOKAN); Formal analysis, S.E.B.K. (Sena Esen BAYER KESKİN) and N.M.T.; Visualization, S.E.B.K. and M.E. (MERVE EFE); Writing—original draft, N.M.T and S.E.B.K.; Writing—review and editing, S.E.B.K. and N.T.T.; Software and Resources, S.E.B.K. and N.T.T.

Declaration of Competing Interest

The authors whose names are listed immediately below certify that they have NO affiliations with or involvement in any organization or entity with any financial interest or non-financial interest in the subject matter or materials discussed in this manuscript.

References

[1] Herrojo, C., Mata-Contreras, J., & Martín, F. (2017). Application of Split Ring Resonator (SRR) Loaded Transmission Lines to the Design of Angular Displacement and Velocity Sensors for Space Applications. IEEE Transactions on Microwave Theory and Techniques, 65(11), 4450–4460.

[2] Wang, X., et al. (2023). MXene-Coated Planar Microwave Resonator Sensor for Ultrasensitive Humidity Monitoring. IEEE Sensors Journal, 23(8), 9042–9050.

[3] Özbey, B., et al. (2014). Microwave Sensor for Detection of Solid Material Permittivity in Single Multilayer Samples with High Quality Factor. Sensors, 14(12), 22671–22683.

[4] Özbey, B., et al. (2016). Wireless Measurement of Elastic and Plastic Deformation by a Metamaterial-Based Sensor. Sensors, 16(10), 19609–19621.

[5] Aydin, C., et al. (2021). Microwave Sensor Loaded with Complementary Curved Ring Resonator for Material Permittivity Detection. IEEE Sensors Journal, 21(12), 13564–13572.

[6] Chen, L., et al. (2021). A Microwave Sensor with Operating Band Selection to Detect Rotation and Proximity in the Rapid Prototyping Industry. IEEE Sensors Journal, 21(3), 3441–3448.

[7] Ebrahimi, A., et al. (2015). Metamaterial-Inspired Rotation Sensor with Wide Dynamic Range. IEEE Sensors Journal, 15(8), 4621–4628.

[8] Naqui, J., & Martín, F. (2013). Alignment and Position Sensors Based on Split Ring Resonators. Sensors, 12(9), 11790–11797.

[9] Naqui, J., & Martín, F. (2014). Angular Displacement and Velocity Sensors Based on Electric-LC (ELC) Loaded Microstrip Lines. IEEE Sensors Journal, 14(4), 939–940.

[10] Horestani, A. K., et al. (2013). Displacement Sensor Based on Diamond-Shaped Tapered Split Ring Resonator. IEEE Sensors Journal, 13(4), 1153–1160.

[11] Yang, W., et al. (2023). An Angular Displacement Microwave Sensor With 360° Dynamic Range Using Multi-Mode Resonator. IEEE Sensors Journal, 23(14), 7214–7222.

[12] Horestani, A. K., et al. (2013). Rotation Sensor Based on Horn-Shaped Split Ring Resonator. IEEE Sensors Journal, 13(8), 3014–3015.

[13] Ozbey, B., et al. (2023). Directional-Coupler-Based Microwave Sensors for Differential Angular-Displacement Measurement. IEEE Sensors Journal, 23(17), 9984–9992.

[14] Maleki Gargari, A., et al. (2018). A Wireless Metamaterial-Inspired Passive Rotation Sensor with Submilliradian Resolution. IEEE Sensors Journal, 18(11), 4482–4489.

[15] Wang, H., et al. (2022). A Conversionless Angular Displacement Antenna Sensor Node Based on Microstrip Cross-Shaped Matching Network with Rotational Stub for RFID Applications. IEEE Transactions on Antennas and Propagation, 70(1), 799–804.

[16] Wang, Y., et al. (2021). Group-Delay-Based Angular-Displacement Microwave Sensor Using Transversal Signal-Interference Principle. IEEE Microwave and Wireless Components Letters, 31(2), 153–156.

[17] Albostan, U., et al. (2020). Detection Modalities of Displacement Sensors Based on Split Ring Resonators: Pros and Cons. Sensors, 20(22), 6703.

[18] Horestani, A. K., et al. (2012). Rotation Sensing Based on the Symmetry Properties of an Open-Ended Microstrip Line Loaded with a Split Ring Resonator. Progress In Electromagnetics Research C, 26, 153–165.

[19] Shen, M., et al. (2023). A Planar Microwave Angular Displacement Sensor Based on Microstrip Line Loaded Split Ring Resonators. IEEE Microwave and Wireless Technology Letters, 33(1), 55–58.

[20] Martín, F., et al. (2023). Planar Microwave Sensors. Wiley-IEEE Press.

[21] Maleki Gargari, A., et al. (2018). A Wireless Metamaterial-Inspired Passive Rotation Sensor with Sub-milliradian Resolution. IEEE Sensors Journal, 18(11), 4482–4489.